


**Variational Bethe ansatz approach for dipolar one-dimensional bosons**S. De Palo<sup>1,2</sup>, R. Citro<sup>3,4</sup> and E. Orignac<sup>5</sup><sup>1</sup>*CNR-IOM-Democritos National Simulation Centre, UDS Via Bonomea 265, I-34136, Trieste, Italy*<sup>2</sup>*Dipartimento di Fisica Teorica, Università Trieste, Strada Costiera 11, I-34014 Trieste, Italy*<sup>3</sup>*Dipartimento di Fisica “E. R. Caianiello” and CNR-SPIN, Università degli Studi di Salerno, Via Giovanni Paolo II, I-84084 Fisciano (Sa), Italy*<sup>4</sup>*INFN, Sezione di Napoli, Gruppo collegato di Salerno, I-84084 Fisciano (Sa), Italy*<sup>5</sup>*Univ Lyon, Ens de Lyon, Univ Claude Bernard, CNRS, Laboratoire de Physique, F-69342 Lyon, France* (Received 10 October 2019; revised manuscript received 9 December 2019; published 6 January 2020)

We propose a variational approximation to the ground state energy of a one-dimensional gas of interacting bosons on the continuum based on the Bethe ansatz ground state wave function of the Lieb-Liniger model. We apply our variational approximation to a gas of dipolar bosons in the single mode approximation and obtain its ground state energy per unit length. This allows for the calculation of the Tomonaga-Luttinger exponent as a function of density and the determination of the structure factor at small momenta. Moreover, in the case of attractive dipolar interaction, an instability is predicted at a critical density, which could be accessed in lanthanide atoms.

DOI: [10.1103/PhysRevB.101.045102](https://doi.org/10.1103/PhysRevB.101.045102)**I. INTRODUCTION**

One-dimensional interacting bosons [1] are a very active topic in current research on the many-body problem, owing to availability of experimental systems and powerful theoretical techniques. One-dimensional bosons with repulsive interactions are expected to have the Tomonaga-Luttinger liquid state [2,3] as the ground state and display simultaneously critical superfluid and density wave fluctuations with interaction dependent exponents. In contrast to the case of fermions [3], these exponents cannot be obtained from perturbation theory in the vicinity of the noninteracting point. Instead, it is necessary to know the dependence of the ground state energy per unit length as a function of particle density [2]. In the case of integrable models [4,5] such dependence can be obtained analytically, but in the general case, one resorts to numerical methods such as quantum Monte Carlo [6,7] or density matrix renormalization group [8]. Variational methods have also been proposed [9–13], using as variational wave function the ground state wave function of the Calogero-Sutherland model [14–18]. With such variational wave functions, the Tomonaga-Luttinger exponent is the variational parameter. This form of variational wave function can be interpreted [19] in terms of a Jastrow [20] factor. Because of the difficulty of computing correlation functions, the use of Bethe ansatz wave functions as variational wave functions has been mainly restricted to few body systems [21,22] in harmonic traps, although a Bethe ansatz density functional theory has been proposed in the case of spin-1/2 fermions in harmonic potential [23,24]. However [25,26], using determinant representations of correlation functions has allowed calculation of the structure factor of Bethe ansatz integrable models. Such developments enable the use of Bethe ansatz wave functions in a variational approach [27]. Moreover, in the case of the integrable Lieb-Liniger [4] gas, an approximation to the exact structure factor [26] is

known that further simplifies the variational calculation in the thermodynamic limit.

Here we introduce a variational approach using the Bethe-ansatz wave functions of the Lieb-Liniger model as variational wave functions to determine the Tomonaga-Luttinger exponents of a one-dimensional interacting model of bosons with a sufficiently short-range interaction. In particular, we apply it to a dipolar gas, using the separation of the dipole-dipole interaction (DDI) in an effective contact potential and a soft long-range part.

This study is particular timely as, recently, highly magnetic lanthanide atoms such as dysprosium and erbium have given access to strong magnetic dipole-dipole interactions (DDI) in ultracold atomic physics [28–31]. The interplay of the short-ranged van der Waals s-wave interaction and the long-range and anisotropy nature of DDI in the atomic gas has enabled the exploration of a wide variety of phenomena. The most recent ones are novel quantum liquids [32–34], strongly correlated lattice states [35–37], exotic spin dynamics [38] and the emergence of thermalization in a nearly integrable quantum gas [39]. An even more exciting physics can be accessed when dimensionality is reduced. In fact in optical lattices, one would be able to create dipolar Tomonaga-Luttinger liquids [7,40] as well as novel quantum phases [41], including analogs of fractional quantum Hall states [42]. On the application side, setting the DDI strength to zero improves the sensitivity of atom interferometry [43], atomtronic devices based on dipolar interactions have been proposed [44], and tuning the interaction strength from positive to negative may find application in the simulation of nuclear matter.

Special attention has been devoted to the strictly one-dimensional case with repulsive interactions, in which both the determination of the equation of state [45] and of the structure factor [46] has suggested the existence of a crossover from a liquidlike, superfluid state with the characteristics

of a Tonks-Girardeau gas [47] to a quasiordered (particles localized at lattice sites), normal-fluid state with increasing the linear density. However, in trapped atom experiments, the finite transverse width of the trap allows an averaging of repulsive and attractive dipolar interactions [40,48] that precludes the formation of the quasiordered state. In the present paper, we wish to understand the crossover from the low density Tonks-Girardeau-like regime to the quasi-BEC regime at high density by studying the evolution of the Tomonaga-Luttinger exponent with an approach applicable to interacting one-dimensional boson models in the continuum. Understanding the interplay between short-range van der Waals and longer ranged interactions remains an experimental challenge that may lead to new physics.

The paper is organized as follows. Section II describes the variational approach for a general setting. Section III introduces a model of dipolar bosons in a transverse harmonic trap [40,48] and discusses the application of the variational approach and the computation of the Tomonaga-Luttinger parameters. In Sec. IV we offer some conclusions and perspectives.

## II. THE VARIATIONAL APPROACH

We consider the full Hamiltonian of a one-dimensional interacting bosonic system

$$H_{1D} = \mathcal{K} + \mathcal{V}, \quad (1)$$

where

$$\mathcal{K} = -\frac{\hbar^2}{2m} \sum_{i=1}^N \frac{\partial^2}{\partial x_i^2}, \quad \mathcal{V} = \sum_{1 \leq i < j \leq N} v(x_i - x_j)$$

with  $v(x)$  a sufficiently short ranged interaction, with Fourier transform  $\hat{v}(k) = \int dx v(x) e^{-ikx}$ , defined for all  $k$ .

We then introduce the variational Hamiltonian:

$$H_{\text{var}} = \mathcal{K} + g\mathcal{U}, \quad (2)$$

where

$$\mathcal{U} = \sum_{1 \leq i < j \leq N} \delta(x_i - x_j)$$

which is a Lieb-Liniger Hamiltonian that is Bethe-ansatz integrable [4,49]. Let  $|\psi_0(g)\rangle$  the ground state wave function of the Lieb-Liniger Hamiltonian (2), such that  $H_{\text{var}}|\psi_0(g)\rangle = E_0(g)|\psi_0(g)\rangle$ .

We re-write the original Hamiltonian (1) in terms of the variational one as

$$H_{1D} = H_{\text{var}} + \mathcal{V} - g\mathcal{U} \quad (3)$$

and use  $|\psi_0(g)\rangle$  as a variational wave function, so that  $E_{\text{var}} = \langle \psi_0(g) | H_{1D} | \psi_0(g) \rangle$  is the variational energy [27] to be minimized as a function of  $g$

$$E_{\text{var}}(g) = E_0(g) + \langle \psi_0(g) | \mathcal{V} - g\mathcal{U} | \psi_0(g) \rangle.$$

The Hellmann-Feynman theorem,  $\frac{\partial E_0(g)}{\partial g} = \langle \psi_0(g) | \mathcal{U} | \psi_0(g) \rangle$ , yields

$$E_{\text{var}}(g) = E_0(g) - g \frac{\partial E_0(g)}{\partial g} + \langle \psi_0(g) | \mathcal{V} | \psi_0(g) \rangle. \quad (4)$$

We then express  $\langle \psi_0(g) | \mathcal{V} | \psi_0(g) \rangle$  in terms of the static structure factor  $S(k)$  (see Appendix A for derivation and definitions) in the ground state  $|\psi_0(g)\rangle$  and obtain the trial energy per unit length  $e_{\text{var}}(g) = E_{\text{var}}(g)/L$ :

$$e_{\text{var}}(g) = e_0(g) - g \frac{\partial e_0(g)}{\partial g} + \frac{n}{2} [n\hat{v}(k=0) + \int_{-\infty}^{\infty} \frac{dk}{2\pi} \hat{v}(k) S(k) - v(x=0)], \quad (5)$$

where  $n = N/L$  is the number of bosons per unit length and  $e_0(g) = E_0(g)/L$  is the Lieb-Liniger energy per unit length.

The calculation of the variational energy requires knowledge of  $e_0(g)$  and the static structure factor  $S(k)$  of the Lieb-Liniger model. The ground-state energy can be obtained from the Bethe ansatz solution [4] by solving an integral equation (see Appendix B). It takes the form

$$e_0(g) = \frac{\hbar^2 n^3}{2m} \epsilon_{LL}(\gamma), \quad (6)$$

with the dimensionless parameter

$$\gamma = \frac{mg}{\hbar^2 n}. \quad (7)$$

Moreover, an analytical conjecture for the exact result for  $\epsilon_{LL}$  is known [50–52] (see Appendix B) and can be readily used to estimate the derivative in Eq. (5). The static structure factor  $S(k)$  has been obtained from the form factor expansion [26] or using Monte Carlo approaches [53] for selected interaction strengths. Later, an analytic expression of  $S(k)$ , interpolating between weak and strong repulsion and in broad agreement with the result of Ref. [26], was proposed [54]. Using that approximation greatly simplifies the evaluation of the trial energy in Eq. (5). Once the optimal  $g$  that minimizes the trial energy has been found, Eq. (5) yields an approximation for the ground state energy per unit length  $e_{GS}$  of the original Hamiltonian.

A one-dimensional interacting system of spinless bosons with repulsive interactions is expected to form a Tomonaga-Luttinger liquid in its ground state [1]. The low-energy excitations of such Tomonaga-Luttinger liquid are described by a bosonized Hamiltonian

$$H_b = \hbar \int \frac{dx}{2\pi} \left[ uK(\pi\Pi)^2 + \frac{u}{K}(\partial_x\phi)^2 \right], \quad (8)$$

where  $u$  is the velocity of excitations and  $K$  the Tomonaga-Luttinger exponent [2]. The latter exponent determines the long distance decay of the single particle Green's function and of the density-density correlations [2] as well as the stability against the formation of a gapped state when an infinitesimal periodic potential commensurate with the density is applied along the tubes [55–57]. The effect of renormalization of the Tomonaga-Luttinger exponent by a finite periodic potential on the phase diagram has been studied in Ref. [57]. As a result of Galilean invariance [2] of (1),

$$uK = \frac{\hbar\pi n}{m}, \quad (9)$$

while [2]

$$\frac{u}{K} = \frac{1}{\pi\hbar} \frac{\partial^2 e_{GS}}{\partial n^2}, \quad (10)$$

where  $e_{GS}(n)$  is the ground state energy per unit length. The existence of the Tomonaga-Luttinger liquid requires  $\frac{\partial^2 e_{GS}}{\partial n^2} > 0$ . The vanishing of  $\frac{\partial^2 e_{GS}}{\partial n^2}$  signals a collapse instability [58,59] towards a state of high (possibly infinite) density. In the next section, we will illustrate the application of this variational method to a gas of one-dimensional dipolar bosons with repulsive contact interaction.

### III. THE QUASI-ONE-DIMENSIONAL DIPOLAR MODEL

The effective Hamiltonian in the single-mode approximation (SMA) [40,48], for polarized bosonic dipoles trapped in quasi-one-dimensional geometry reads:

$$H_{\text{Q1D}} = -\frac{\hbar^2}{2m} \sum_i \frac{\partial^2}{\partial x_i^2} + \sum_{i<j} V_{\text{Q1D}}(x_i - x_j) + g_{v,dW} \sum_{i<j} \delta(x_i - x_j) \quad (11)$$

where, compared to Hamiltonian (1) we have two contributions to the two-body potential energy:  $V_{\text{Q1D}}(x)$  is the effective 1D dipole-dipole interaction obtained after projection of the transverse degrees of freedom [40,48] and  $g_{v,dW}\delta(x)$ , which originates from the Van der Waals interaction and other short range interatomic interactions. These latter interactions are represented in three dimensions by the Huang-Yang pseudopotential [60,61]. After projection of the transverse degrees of freedom, the pseudopotential yields the one-dimensional contact interaction with [61]  $g_{v,dW} = \frac{2\hbar^2 a_{3D}}{ml_{\perp}^2} (1 - C \frac{a_{3D}}{\sqrt{2}l_{\perp}})^{-1}$  where  $a_{3D}$  is the s-wave scattering length of the three-dimensional short range potential,  $l_{\perp} = \sqrt{\hbar/(m\omega_{\perp})}$  is the transverse trapping length, and  $C = 1.4603 \dots$  is a numerical constant. Away from the confinement induced resonance,  $a_{3D} \ll l_{\perp}$ , the single mode approximation is applicable, and one can approximate

$$g_{v,dW} = \frac{2\hbar^2 a_{3D}}{ml_{\perp}^2}. \quad (12)$$

If one wished to include confinement induced resonances, it would be necessary to include the van der Waals and the dipolar interaction in a single Huang-Yang pseudopotential [62]. Such treatment is beyond the scope of our paper.

In the Hamiltonian Eq. (11), the effective 1D dipole-dipole interaction is [40,48]

$$V_{\text{Q1D}}(x) = V(\theta) \left[ V_{\text{DDI}}^{\text{1D}} \left( \frac{x}{l_{\perp}} \right) - \frac{8}{3} \delta \left( \frac{x}{l_{\perp}} \right) \right], \quad (13)$$

$$V(\theta) = \frac{\mu_0 \mu_D^2}{4\pi} \frac{1 - 3 \cos^2 \theta}{4l_{\perp}^3}, \quad (14)$$

$$V_{\text{DDI}}^{\text{1D}} \left( \frac{x}{l_{\perp}} \right) = -2 \left| \frac{x}{l_{\perp}} \right| + \sqrt{2\pi} \left[ 1 + \left( \frac{x}{l_{\perp}} \right)^2 \right] \times e^{\frac{1}{2} \left( \frac{x}{l_{\perp}} \right)^2} \text{erfc} \left[ \left| \frac{x}{\sqrt{2}l_{\perp}} \right| \right], \quad (15)$$

where  $\mu_0$  is the magnetic permeability of the vacuum,  $\mu_D$  is the magnetic dipolar moment of the atom ( $\mu_D = 9.93 \mu_B$  in the case [39] of  $^{162}\text{Dy}$ ), and  $\theta$  is the angle of the dipoles with

respect to the  $x$  axis. The Fourier transform of the soft-dipolar interaction  $V_{\text{DDI}}^{\text{1D}}(r/l_{\perp})$  reads [40]:

$$\hat{V}_{\text{DDI}}(k) = 4l_{\perp} \left[ 1 - \frac{(kl_{\perp})^2}{2} e^{-\frac{(kl_{\perp})^2}{2}} E_1 \left( \frac{(kl_{\perp})^2}{2} \right) \right], \quad (16)$$

where  $E_1(x) = \Gamma(0, x)$  is the exponential integral function [63].

We can divide the Hamiltonian, Eq. (11), into a Lieb-Liniger part that contains all the contact interactions and the rest, a nonintegrable soft-dipolar part. The Lieb-Liniger part of the Hamiltonian then reads:

$$H_{\text{Q1D}}^{\text{LL}} = -\frac{\hbar^2}{2m} \sum_i \frac{\partial^2}{\partial x_i^2} + g_{\text{Q1D}}(\theta) \sum_{i<j} \delta(x_i - x_j)$$

where  $g_{\text{Q1D}}(\theta) = [g_{v,dW} - V(\theta) \frac{8}{3} l_{\perp}]$ . The dimensionless parameter  $\gamma_0$  associated to  $g_{\text{Q1D}}(\theta)$  is given by:

$$\gamma_0 = \frac{1}{n} \frac{m}{\hbar^2} g_{\text{Q1D}}(\theta) = \frac{2}{na_{\text{Q1D}}} = \gamma_{v,dW} + \gamma_d = \frac{2}{n} \left[ -\frac{1}{a_{\text{1D}}} - 4 \frac{a_d}{l_{\perp}^2} \frac{1 - 3 \cos^2 \theta}{3} \right] \quad (17)$$

where we have introduced the dipole length scale  $a_d$  for the one-dimensional dipolar interaction, as defined in Ref. [64], which for the  $^{162}\text{Dy}$  atoms is  $a_d = \frac{\mu_0 \mu_D^2 m}{8\pi \hbar^2} \simeq 195a_0$  where  $a_0$  is the Bohr radius. In the following, we will treat  $a_{\text{1D}}$  as a phenomenological parameter measuring the strength of the short range interaction. This value can be converted into a three-dimensional interaction using the approximation of Eq. (12).

The original Hamiltonian, Eq. (11), can therefore be written as the sum of the Lieb-Liniger part and the rest:

$$H = H_{\text{Q1D}}^{\text{LL}}(\gamma_0) + V(\theta) \sum_{i<j} V_{\text{DDI}}^{\text{1D}} \left( \frac{x_i - x_j}{l_{\perp}} \right). \quad (18)$$

We can now use a variational Hamiltonian of the form Eq. (2), in which the contact interaction contains already the short range part of (11), and minimize the trial ground state energy (5). The variational contact interaction is written  $g = g_{\text{Q1D}}(\theta) + \bar{g}$ , with  $\bar{g}$  to be determined by minimization.

Following Sec. II, we can extract the optimal correction to  $g_0 = g_{\text{Q1D}}(\theta)$  by minimizing the trial energy per particle written in terms of dimensionless ratios  $a_d/l_{\perp}$ ,  $nl_{\perp}$  and the adimensional parameter  $\gamma = \frac{1}{n} \frac{m}{\hbar^2} [g_{\text{Q1D}}(\theta) + \bar{g}] = \gamma_0 + \bar{\gamma}$  with respect to  $\bar{\gamma}$

$$\begin{aligned} \frac{2mE}{N\hbar^2 n^2} &= \epsilon(\gamma) - \bar{\gamma} \frac{\partial \epsilon(\gamma)}{\partial \gamma} + 2 \frac{a_d}{l_{\perp}} \frac{1 - 3 \cos^2 \theta}{nl_{\perp}} \\ &\times \left\{ 1 + \int_0^{\infty} dq [S(\pi q n; \gamma) - 1] \right. \\ &\times \left. \left[ 1 - \frac{\pi^2 q^2 n^2 l_{\perp}^2}{2} e^{-\frac{\pi^2 q^2 n^2 l_{\perp}^2}{2}} \Gamma \left( 0, \frac{\pi^2 q^2 n^2 l_{\perp}^2}{2} \right) \right] \right\}, \end{aligned} \quad (19)$$

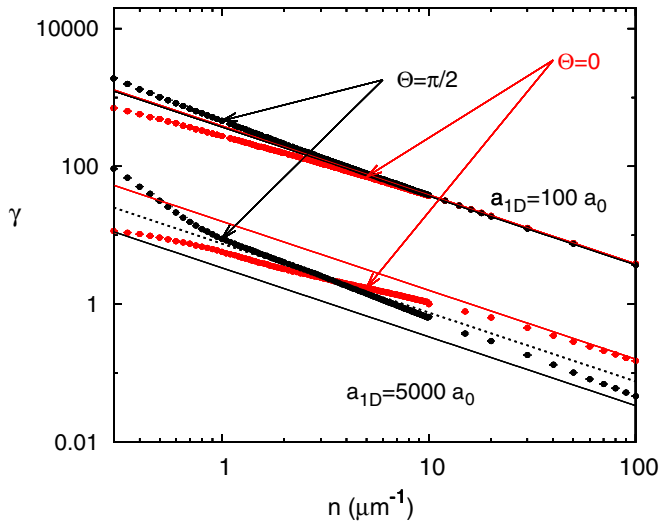


FIG. 1.  $\gamma$  as a function of  $n$  for two values of the scattering length for contact interaction  $a_{1D}$ . Solid lines represent  $\gamma_0$  from Eq. (17) at angles  $\theta = 0$  (red) and  $\theta = \frac{\pi}{2}$  (black). The dashed (black) line represents  $\gamma_{vdW}$ . The diamonds represent the optimal  $\gamma$  obtained by minimizing Eq. (19), for angle  $\theta = 0$  (red) and  $\theta = \frac{\pi}{2}$  (black). At large density,  $\gamma$  admits  $\gamma_0$  as asymptote.

where  $q$  is dimensionless. Using for instance the golden search algorithm [65] or simply scanning the energy as a function of  $\bar{\gamma}$  it is possible to find the minimum of Eq. (19). The optimal  $\gamma$ , obtained through the minimization procedure, depends on three independent dimensionless parameters, such as  $na_{1D}$ ,  $a_{1D}/l_{\perp}$ , and  $a_d(1 - 3 \cos^2 \theta)/l_{\perp}$ . At the critical angle

$$\theta_c = \arccos\left(\frac{1}{\sqrt{3}}\right) \quad (20)$$

the optimal  $\gamma$  coincides by construction with  $\gamma_0$  and depends only on  $na_{1D}$ . At large densities (see Appendix D) the contribution of the dipolar interactions in Eq. (19) is depressed by the  $1/(nl_{\perp})$  factor together with the decay of  $\hat{V}(q\pi nl_{\perp}) \sim 2/(q\pi nl_{\perp})^2$ , so that upon minimization  $\gamma \rightarrow \gamma_0$  asymptotically, as if the dipolar interaction was reduced to its contact contribution. If we consider Eq. (17) the contribution of the contact term  $\gamma_d$  due to dipolar interactions is independent of density  $n$ , positive when  $\theta < \theta_c$  and negative for  $\theta > \theta_c$ , up to a point where  $\gamma_0$  can change its sign and become negative. In such a case, the Tomonaga-Luttinger liquid state should be unstable at high density. By contrast, for low densities, the noncontact contribution of the dipolar interactions to the variational energy is enhanced, and overwhelms the contact term. The optimal  $\gamma$  is enhanced when  $\theta > \theta_c$  and lowered when  $\theta < \theta_c$  (see Appendix C).

In Fig. 1 we show the dependence of  $\gamma$  (solid dots) on the density  $n$  for two selected cases,  $a_{1D} = 100a_0$  and  $a_{1D} = 5000a_0$ , and two angles,  $\theta = 0$  and  $\theta = \pi/2$ . For comparison the value of  $\gamma_0$  (solid lines) from Eq. (17) are shown, as well as  $\gamma_{vdW} = 2/(na_{1D})$  (dashed lines). When not stated explicitly all results refer to estimates where we have taken  $a_d = 195a_0$  and  $l_{\perp} = 57.3 \text{ nm}$  [39].

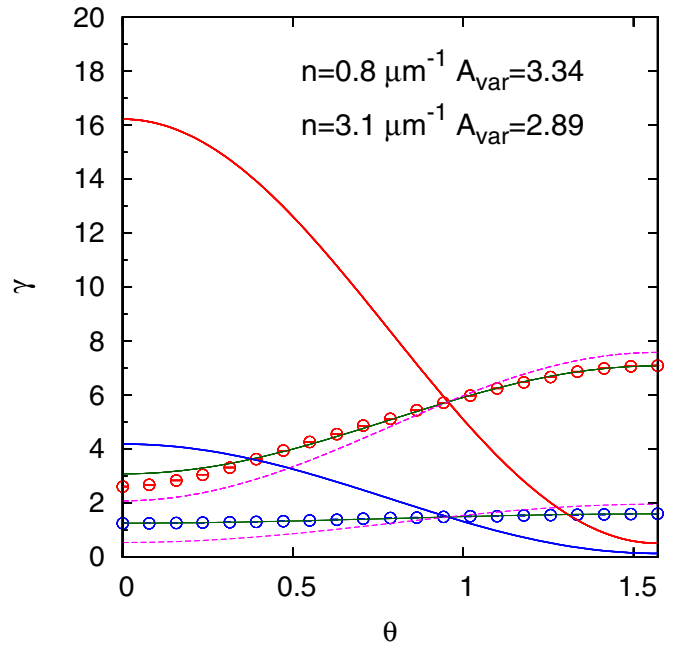


FIG. 2.  $\gamma$  as a function of  $\theta$  for  $n = 0.8 \mu\text{m}^{-1}$  red curves, and for  $n = 3.1 \mu\text{m}^{-1}$ , blue curves. Solid curves represent  $\gamma_0$  while open dots are the results of the minimization procedure. The dashed magenta lines are the estimates for  $\gamma$  if we use Eq. (21) with  $A = 3.6$  for both densities [39], while the dark-green lines fits of the variational estimates to an expression of the form (21) with  $n$  dependent values of  $A$  indicated in the inset.

In Ref. [39], the dipolar interaction is approximated by replacing the full interaction (15) by  $g_{1D}^{\text{total}}\delta(x)$  where:

$$g_{1D}^{\text{total}} = g_{vdW} + V(\theta)l_{\perp}\left(A - \frac{8}{3}\right)\delta(x)$$

$$A = \int_{-\sqrt{2\pi}}^{\sqrt{2\pi}} du V_{\text{DDI}}^{\text{1D}}(u),$$

the integration bounds being chosen so that  $A = 3.6$  is 90% of the exact integral  $\hat{V}_{\text{DDI}}(k=0)/l_{\perp}$ . Analogously to our variational approach the dipolar interaction is replaced by a simpler contact interaction. However, the criteria used to define the contact interaction are markedly different. In Ref. [39], the potential is replaced by a  $\delta$ -function potential having almost the same Fourier transform at  $k=0$ . Such approximation is expected to be valid when the interparticle distance is large compared with  $l_{\perp}$ , i.e., when  $nl_{\perp} \ll 1$ . In our variational approach, no assumption is made on the two-particle scattering problem nor interparticle distance, since the effective contact interaction is determined by the minimization of the energy per particle. At low density,  $nl_{\perp} \ll 1$ , it should be possible to make contact with the approximation of Ref. [39] and we should have

$$\bar{g} \rightarrow A_{\text{var}}V(\theta)l_{\perp}, \quad (21)$$

where  $A_{\text{var}}$  is a dimensionless constant. The values of  $A_{\text{var}}$  we find (see Fig. 2) are in reasonable agreement with the approximations used in Ref. [39]. However, the coefficient  $A_{\text{var}}$  in Eq. (21) that gives the best fit to the variational value of

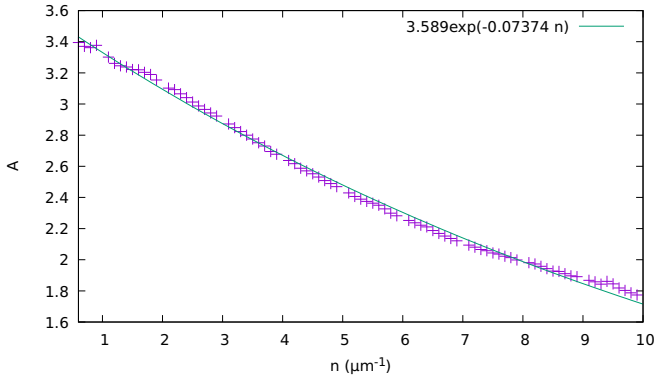


FIG. 3. Behavior of  $A$  obtained by fitting the variational  $\gamma$  to an expression of the form (21) for a given density  $n$ . The amplitude  $A$  is seen to decrease approximately exponentially with  $n$ , reaching a value of order 3.6 at low density.

$\gamma$  decreases slightly with  $n$ . In Fig. 3, we show the dependence of  $\tilde{A}$  obtained by fitting the  $\theta$  dependence of the optimal  $\gamma$  with an expression of the form (21). We find that the dependence can be described by an exponential and that at low density the result of Ref. [39] holds.

The minimum of the trial energy per particle, Eq. (19), in units of  $\frac{\hbar^2 n^2}{2m}$  is  $\epsilon_{\text{var}}(n)$ , and can be expressed as

$$\epsilon_{\text{var}}(n) = \epsilon_{LL}[\gamma_0(n)] + \Delta\epsilon(n) \quad (22)$$

where  $\epsilon_{LL}(\gamma_0(n))$  is the dimensionless Lieb-Liniger ground-state energy defined in Eq. (6) at dimensionless parameter  $\gamma_0(n)$  [see Eq. (17)] while the contribution of the nonintegrable soft-dipolar interaction is encapsulated in the  $\Delta\epsilon(n)$  correction.

As discussed before, at large density the  $\gamma \rightarrow \gamma_0$  and  $\epsilon_{\text{var}}(n) \rightarrow \epsilon_{LL}(\gamma_0(n))$ . At small density, whenever the optimal  $\gamma$  is so large that we can approximate the static structure factor as the one of the noninteracting fermionic gas, the correction due the soft dipolar interaction  $\Delta\epsilon(n) \propto n \log(n)$  (see Appendix D for a detailed discussion). This behavior can be seen in Fig. 4 where the  $\Delta\epsilon(n)$  corrections are shown as a function of density for  $a_{1D} = 100a_0$ . At large density as well as for small density these corrections go to zero, in the inset we show  $\Delta\epsilon(n)/(n \log(n))$  that for extremely low density goes towards a constant value.

#### A. $\theta > \theta_c$ : Repulsive soft dipolar interaction

As already observed, the overall effect of the repulsive soft dipolar interaction is to make the optimum  $\gamma(n) > \gamma_0$ . In the large density limit,  $nl_{\perp} \gg 1$ ,  $\gamma \rightarrow \gamma_0$  and according to Eq. (17), we can find  $\gamma_0 < 0$  if

$$a_d > \frac{3l_{\perp}^2}{4|a_{1D}|(1 - 3\cos^2\theta)}. \quad (23)$$

If that condition is satisfied, the dipolar gas is unstable at high density. Otherwise, the gas is stable for all densities. In Fig. 5 we show  $\epsilon_{\text{var}}(n)$ ,  $\epsilon_{LL}[\gamma_0(n)]$  together with  $\epsilon_{LL}[\gamma(n)]$ , for various scattering length  $a_{1D}$  as a function of the density. At very low density the Tonks-Girardeau limit  $\epsilon(n) = \pi^2/3$  is recovered, while in the very high density limit the weakly

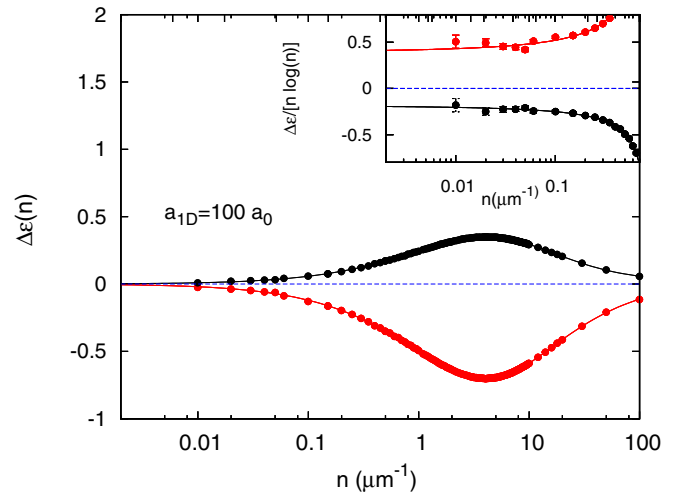


FIG. 4. Plot of  $\Delta\epsilon(n)$  from Eq. 22 as a function of atom density for  $a_{1D} = 100a_0$  for  $\theta = 0$  (red solid dots) and  $\theta = \pi/2$  (black solid dots). The red and black solid lines are fitting curves of the form:  $f(n) = (an \log n + bn^{5/4} + cn^2)/(1 + dn + e^{2+\delta})$ . When  $\theta = 0$  we get  $a = 0.394(3)$ ,  $b = -0.551(6)$ ,  $c = -0.009(2)$ ,  $d = 0.13(1)$ ,  $e = 0.00039(8)$ ,  $g = 1.14(1)$ ; when  $\theta = \pi/2$  we get  $a = -0.1853(2)$ ,  $b = 0.287(1)$ ,  $c = -0.00136(4)$ ,  $d = 0.168(5)$ ,  $e = -0.0005(1)$ ,  $g = 0.73(3)$ . In the inset we show the low density behavior of  $\Delta\epsilon(n)/(n \log n)$  with the same color code.

interacting regime is recovered. The quantities  $\epsilon_{LL}[\gamma_0(n)]$  and  $\epsilon_{LL}[\gamma(n)]$ , solid and dashed lines in Fig. 5, respectively, can be seen as successive approximations to the variational energies (solid dots). In Fig. 5 we have also shown the case ( $a_{1D}/a_0 = 10000$ , black data) where, for the parameters chosen to make the calculation,  $\gamma_0(n) < 0$  so the condition (23) is met. In

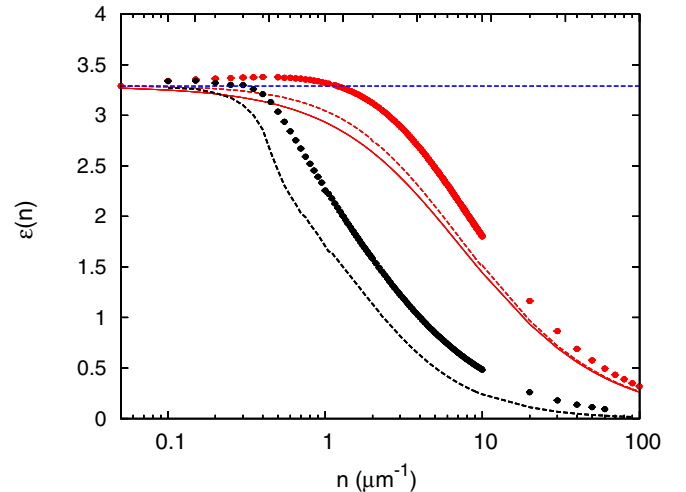


FIG. 5. Plot of energy per particle  $\epsilon(n)$  as a function of atom density, at  $\theta = \pi/2$  corresponding to the largest repulsive soft dipolar interaction, for two scattering length  $a_{1D}/a_0 = 1000$  and  $10000$ ; red and black solid dots, respectively. With the same color code the  $\epsilon_{LL}[\gamma_0(n)]$  (solid line) and  $\epsilon_{LL}[\gamma(n)]$  (dashed line) are shown.  $\epsilon_{LL}[\gamma_0(n)]$  for  $a_{1D}/a_0 = 10000$  is not shown since for the parameter we have chosen  $\gamma_0(n) < 0$ . The dashed blue line represents the low density limit  $\pi^2/3$ .

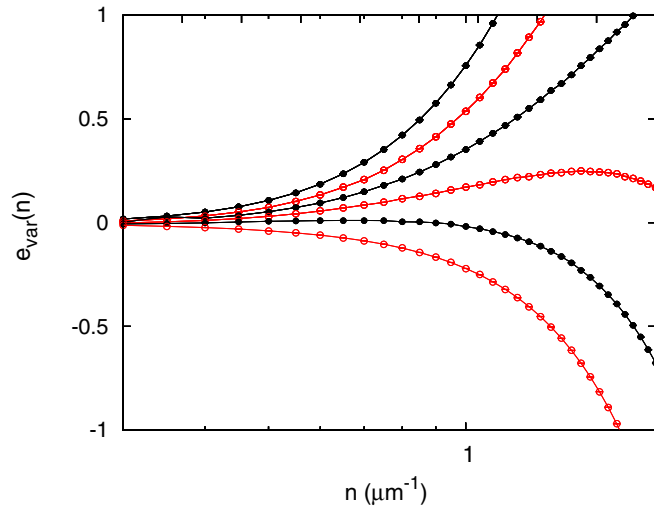


FIG. 6. Plot of energy per unit length as a function of atom density for selected scattering lengths. Starting from the top  $a_{1D}/a_0 = 5000, 6000, 7000, 8000, 9000,$  and  $10000$  for fixed angle  $\theta = 0$ .

the minimization procedure, for the densities considered, we always get a positive optimal  $\gamma$ .

### B. $\theta < \theta_c$ : Attractive soft dipolar interaction

When  $V(\theta)$  is negative,  $\gamma_0$  is enhanced by the contact contribution and the effect of the soft dipolar interaction is to lessen this repulsion. For small scattering lengths, the situation is similar to the one described for the repulsive case but with a negative correction with respect to  $\epsilon_{LL}[\gamma_0(n)]$  in Eq. (22).

However for large scattering lengths at small angles, when the effect of the soft dipolar interaction is larger the system can become unstable. In Fig. 6 we show the variational ground state energy per unit length  $e_{\text{var}}(n)$  for different increasing scattering lengths. When  $a_{1D}/a_0 > 8000$  the energy per unit length is convex at low density but presents a concavity at higher density. In such a case, the compressibility becomes negative, indicating an instability towards collapse at  $n = n_c$  where the second derivative of energy per unit length as a function of density is vanishing.

### C. Tomonaga-Luttinger parameters

Having obtained the ground state energy per unit length, with Eqs. (9) and (10) we can calculate the Tomonaga-Luttinger exponent  $K$  as well as the velocity of excitations  $u$  that enter the bosonized Hamiltonian Eq. (8). At very low density the Tomonaga-Luttinger exponent has a logarithmic correction that qualitatively can be understood as follows (see also Appendix D). In the limit of low density, one can approximate

$$e_{GS} \simeq \frac{\pi^2 n^3}{6m} + \frac{n^2}{2} \hat{v}(k=0) + \int_0^{2\pi n} \frac{dk}{2\pi} \hat{v}(k) \left( \frac{k}{2\pi} - n \right), \quad (24)$$

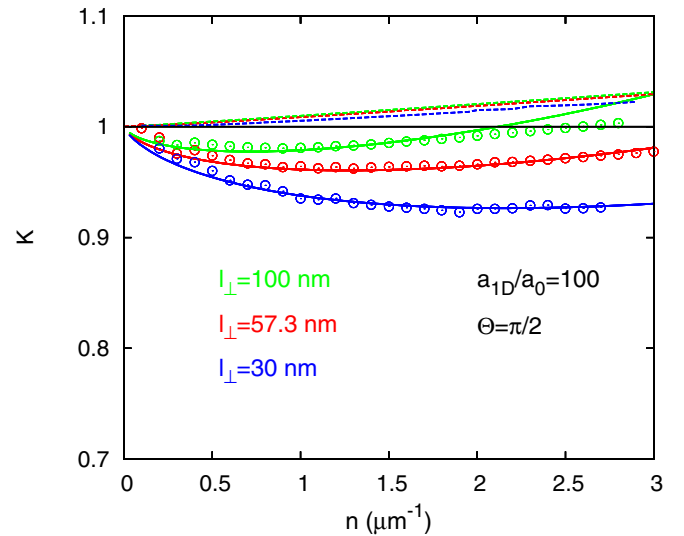


FIG. 7. Plot of the Tomonaga-Luttinger exponent  $K$  deduced from the variational ground state energy in case of maximally repulsive dipolar interaction at  $a_{1D}/a_0 = 100$  for three different values of confinement:  $l_{\perp} = 100, 57.3,$  and  $30$  nm (blue, red, and green data, respectively). Open dots are  $K$  obtained from  $e_{\text{var}}(n)$  by numerical differentiation, solid curves are  $K$  obtained by differentiating the fitted expression  $e(n) = n^3(\pi^2/3 + an \log n + bn^c)$ . The dashed curves are the Tomonaga-Luttinger exponents of the Lieb-Liniger gas computed at the optimal  $\gamma$ .

where we have used Eq. (B14), giving

$$K \simeq \frac{1}{\sqrt{1 + \frac{m}{\pi^2 n} [\hat{v}(0) - \hat{v}(2\pi n)]}}. \quad (25)$$

In the case of dipolar forces [48],  $v(x)$  behaves for long distance distance as  $\sim |x|^{-3}$ , so  $\hat{v}(0) - \hat{v}(2\pi n) \sim n^2 |\ln n| + O(n^2)$ , leading to  $K - 1 \sim n |\ln n|$ . This low density behavior can be traced in  $K$  when  $\gamma$  minimizing the variational energy is sufficiently large to satisfy the above conditions. See for example Fig. 7, where  $K(n)$  obtained by fitting the low density behavior of the  $e_{\text{var}}(n)$ , including a logarithmic correction (solid line) with an expression  $e(n) = n(\pi^2/3 + an \log n + bn^c)$ , is in agreement with the values obtained by numerical differentiation (open dots).

When the dipolar interaction is repulsive, the Tomonaga-Luttinger exponent is lower than the exponent of a Lieb-Liniger gas having either  $\gamma = \gamma_0$  or  $\gamma$  minimizing the variational energy (19). This shows that the contribution from nonintegrable soft dipolar interaction in (18) is not negligible and that it is not correctly approximated by replacing the non-contact interaction in (18) by an effective contact interaction only.

Moreover, such approximations always lead to a Tomonaga-Luttinger exponent larger than unity [54], and as we will see below, the dipolar gas can have a Tomonaga-Luttinger exponent less than unity. Reducing  $l_{\perp}$  with fixed  $r$ ,  $V_{\text{DDI}}(r/l_{\perp}) \rightarrow (l_{\perp}/r)^3$  while  $V(\theta)$  increases as  $l_{\perp}^{-3}$ . As the contribution to the ground-state energy is enhanced, the Tomonaga-Luttinger exponent is progressively reduced and for small density it can be less than unity like in the strictly one-dimensional dipolar gas dipolar gas

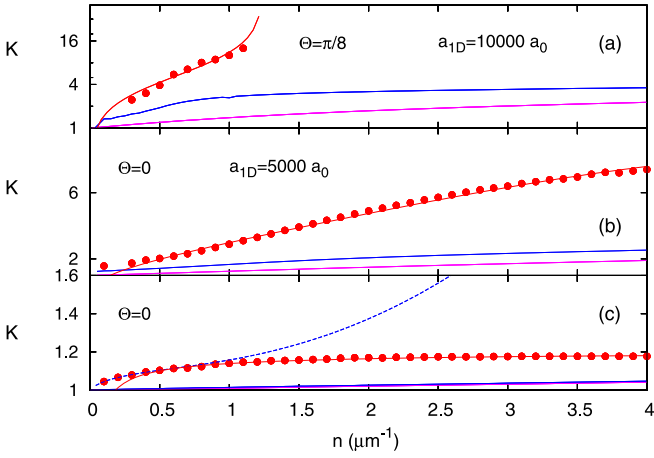


FIG. 8. Plot of the Tomonaga-Luttinger exponent  $K$  derived from variational ground state energy in case of attractive dipolar interaction:  $\theta < \theta_c$ . Red solid dots represent  $K$  obtained from  $e_{\text{var}}(n)$  by numerical differentiation, solid red curve  $K$  obtained using a six degrees polynomial fit for the variational ground state energy and analytic differentiation. Blue and magenta solid curves are the Tomonaga-Luttinger exponents of a Lieb-Liniger gas computed, respectively, at the optimal  $\gamma$  and at  $\gamma_0$ . In panel (a) the results are for  $a_{1D} = 10000a_0$  and  $\theta = \pi/8$  while in both panels (b) and (c)  $\theta = 0$  with  $a_{1D} = 5000a_0$  and  $a_{1D} = 100a_0$ , respectively. The blue dashed curve in panel (c) is a fit of the exponent obtained by numerical differentiation of  $e_{\text{var}}(n)$  to an expression including logarithmic correction.

[7,46,66,67]. In Fig. 7 we show  $K(n)$  for a fixed  $a_{1D}/a_0 = 100$  at  $\theta = \pi/2$ , varying the confinement: namely  $l_{\perp} = 100, 57.3,$  and  $30$  nm. This is a clear indication that approximating the Tomonaga-Luttinger exponent of the dipolar gas with the exponent of a Lieb-Liniger gas can lead to results incorrect not just quantitatively but also qualitatively. Indeed, finding a Tomonaga-Luttinger exponent  $1/2 < K < 1$  yields [3]  $S(k \simeq 2\pi n) \simeq S(2\pi n) + C|k - 2\pi n|^{2K-1} + o(|k - 2\pi n|^{2K-1})$ , giving a cusp in  $S(k)$  near  $k = 2\pi n$ , whereas such a cusp is absent with  $K > 1$ . However, the dynamical superfluid susceptibility remains divergent as long as  $K > 1/4$ .

In the attractive case, the Tomonaga-Luttinger exponent, which is related to the compressibility by Eq. (10), diverges when the homogeneous ground state becomes unstable. In Fig. 8 in panel (a), for  $a_{1D} = 10000a_0$  we show the case in which the system undergoes an instability with  $K$  diverging at  $n_c \sim 1.2 \mu\text{m}^{-1}$ . Panels (b) and (c), for  $a_{1D}/a_0 = 5000$  and  $100$ , respectively, show instead the enhancement of  $K$  due the attractive interaction with respect to the approximations using the Tomonaga-Luttinger exponent of the Lieb-Liniger gas at the optimal  $\gamma$  or at  $\gamma_0$ . Moreover, when  $a_{1D}/a_0 = 100$ , the optimal  $\gamma$  corresponds to the Tonks-Girardeau limit (very low density), and the logarithmic correction to the exponent is visible [see panel (c) where the blue dashed line is obtained by fitting the variational energy taking into account  $n \log(n)$  term, while a six degrees polynomial fit for the variational ground state energy gives results that do not match with the values of  $K(n)$  obtained with numerical differentiation). In Fig. 9 we follow the behavior of the Tomonaga-Luttinger exponent, at fixed density  $n = 1.5 \mu\text{m}^{-1}$  and fixed  $a_{1D} = 10000a_0$ , as a

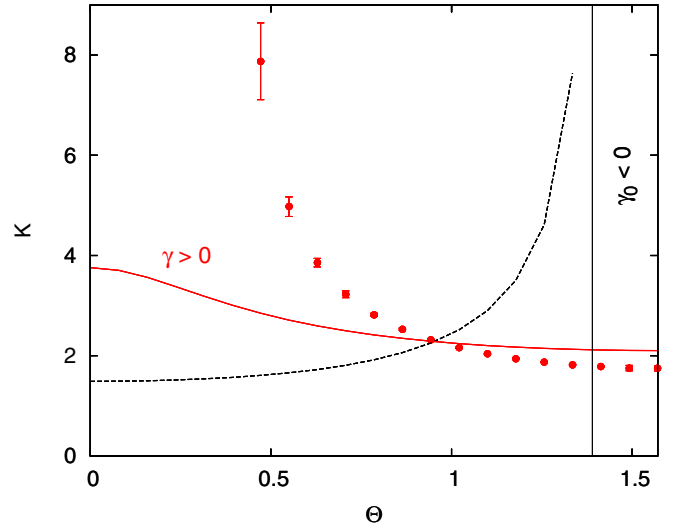


FIG. 9. Plot of the Tomonaga-Luttinger exponent  $K$  deduced from the variational ground state energy as a function of  $\theta$  at fixed density  $n = 1.5 \mu\text{m}^{-1}$ , and scattering length  $a_{1D}/a_0 = 10000$ . A region of instability is found for  $\theta_c < \pi/8$ . The solid red points represent  $K$  obtained from  $e_{\text{var}}(n)$  by numerical differentiation, the solid red curve represents the Tomonaga-Luttinger exponents of the Lieb-Liniger gas computed at the optimal  $\gamma$ . The black dashed curve is  $K$  in the Lieb-Liniger gas at  $\gamma_0$ .

function of the angle  $\theta$ . This is a case where the original  $\gamma_0$  is negative for large angles, while the optimal  $\gamma$  is positive in the whole range of  $\theta$ . However corrections beyond  $e_{LL}(\gamma_{\text{var}})$  predict an instability for  $\theta < \pi/8$ , as shown by the diverging  $K(n)$  corresponding to a change of sign in  $\partial_n^2 e_{\text{var}}(n)$ ; qualitatively, the Tomonaga-Luttinger exponent of a Lieb-Liniger gas with the optimal  $\gamma$  is a decreasing function of  $\theta$  not showing any hint of instability. Moreover, the exponent that would be obtained by neglecting the non Lieb-Liniger part of Eq. (18) is an increasing function of  $\theta$  and shows the instability for  $\theta > \frac{\pi}{3}$ .

#### IV. CONCLUSION

We have presented a variational approach to the ground state energy of bosons in the continuum interacting by a two-body potential, based on analytic expressions for the ground state energy [50] and structure factor [54] of the Lieb-Liniger model. Using this variational approach we have calculated the ground-state energy bosonic atoms in transverse harmonic trapping with dipolar interaction [39] treated within the single mode approximation as a function of density for several scattering lengths, confinement lengths, and spanning the angle of dipoles. From the ground-state energy we have estimated the Tomonaga-Luttinger exponent as a function of density and interaction: When dipolar interactions are attractive and density is sufficiently high an instability of the Tomonaga-Luttinger liquid is predicted. Knowledge of the dependence of the variational ground state energy on the density will permit us to consider the effect of longitudinal harmonic trapping, in particular to compute the frequencies of the breathing modes [68–71]. This will be the object of a future work. The variational method can be applied to other systems of interest

such as atoms interacting via shoulder potentials [72] or power law interactions [73]. The variational approach of the present paper could be extended in different directions. Since an exact form factor representation for the structure factor [26] of the Lieb-Liniger model is available, the Tomonaga-Luttinger exponent and critical density could be calculated more accurately, albeit with greater computational cost with respect to the semianalytical approach presented here. Second, the variational principle used here can be generalized to positive temperature [74] and the free energy of integrable models can be obtained from the thermodynamic Bethe ansatz [75]. Using form factor expansion techniques, the static structure factor of the Lieb-Liniger gas has been calculated for positive temperatures [76], thus the present variational approach could also be generalized to free energy calculations for positive temperatures.

### ACKNOWLEDGMENTS

We thank B. Lev for discussions that inspired this project, and Z. Ristivojevic, L. Sanchez-Palencia, and R. Oldziejewski for comments on the manuscript. E.O. thanks SISSA and Università di Trieste for hospitality.

### APPENDIX A: CONTRIBUTIONS TO THE VARIATIONAL ENERGY

Writing explicitly the average by introducing  $\rho(x) = \sum_{i=1}^N \delta(x - x_i)$  and  $n = N/L$ , being  $N$  the number of particles and  $L$  the system length, one has

$$\langle \psi_0(g) | \mathcal{V} | \psi_0(g) \rangle = \frac{Ln^2}{2} \int dx v(x) g(x) \quad (\text{A1})$$

where  $g(x)$  is the pair correlation function  $n^2 g(x) = \langle \psi_0(g) | \rho(x) \rho(0) | \psi_0(g) \rangle - \frac{N}{L} \delta(x)$ . In the integral (A1), one can introduce the static structure factor  $S(k)$  with

$$g(x) = 1 + \int_{-\infty}^{\infty} \frac{dk}{2\pi n} e^{ikx} [S(k) - 1], \quad (\text{A2})$$

where the relation is derived by the definition of the static structure factor:

$$S(q) = \frac{1}{n} \int_{-\infty}^{+\infty} dx e^{-iqx} [\langle \rho(x) \rho(0) \rangle - n^2], \quad (\text{A3})$$

so that the following relation between the static structure factor and the pair correlation function holds:

$$S(q) = 1 + n \int_{-\infty}^{+\infty} [g(x) - 1] e^{-iqx} dx \quad (\text{A4})$$

and hence:

$$\frac{\langle \psi_0(g) | \mathcal{V} | \psi_0(g) \rangle}{L} = \frac{n}{2} \int_0^{+\infty} \frac{dq}{\pi} \hat{v}(k) [S(q) - 1] + \frac{n^2}{2} \hat{v}(q=0), \quad (\text{A5})$$

where we have used the parity  $S(q) = S(-q)$  and  $\hat{v}(q) = \hat{v}(-q)$ .

The other contribution to the variational energy is evaluated using the Hellmann-Feynman theorem. One can show

that in the Lieb-Liniger model,

$$\frac{\langle \psi_0(g) | \mathcal{U} | \psi_0(g) \rangle}{L} = \frac{n^2}{2} \epsilon'(\gamma), \quad (\text{A6})$$

where

$$\epsilon'(\gamma) = g(0). \quad (\text{A7})$$

### APPENDIX B: GROUND STATE ENERGY AND STATIC STRUCTURE FACTOR OF THE LIEB-LINIGER GAS

We can express the ground state energy  $e_0(g)$  as a function of the dimensionless parameter  $\gamma = \frac{mg}{\hbar^2 n}$  so that  $e_0(g) = \frac{\hbar^2 n^3}{2m} \epsilon_{LL}(\gamma)$ . The function  $\epsilon$  is given by the solution of integral equations [4]

$$2\pi \rho(\mu) = 1 + 2c \int_{-q_0}^{q_0} d\mu' \frac{\rho(\mu')}{c^2 + (\mu - \mu')^2}, \quad (\text{B1})$$

$$n = \int_{-q_0}^{q_0} d\mu \rho(\mu), \quad (\text{B2})$$

$$n^3 \epsilon_{LL}(\gamma) = \int_{-q_0}^{q_0} d\mu \mu^2 \rho(\mu), \quad (\text{B3})$$

where  $c = \frac{mg}{\hbar^2} = n\gamma$ .

In our paper, instead of solving the integral equations (B1) and (B2) we will use the approximate analytical expression for the dimensionless energy  $\epsilon_{LL}(\gamma)$  suggested in Ref. [50]. At small  $\gamma$  where the Lieb-Liniger energy  $\epsilon_{LL}$  is approximated by [50]

$$\begin{aligned} \epsilon_{LL}(\gamma) = \gamma - \frac{4}{3\pi} \gamma^{3/2} + \left[ \frac{1}{6} - \frac{1}{\pi^2} \right] - 0.002005 \gamma^{5/2} \\ + 0.000419 \gamma^3 - 0.000284 \gamma^{7/2} + 0.000031 \gamma^4, \end{aligned} \quad (\text{B4})$$

while from strong to intermediate coupling regime [50]

$$\begin{aligned} \frac{\epsilon_{LL}(\gamma)}{\epsilon^{TG}} = \frac{\gamma^2}{(2+\gamma)^2} + \sum_{n=1}^{\infty} \frac{\pi^{2n} \gamma^2}{(2+\gamma)^{3n+2}} \mathcal{L}_n \\ \mathcal{L}_1 = \frac{32}{15} \\ \mathcal{L}_2 = -\frac{96}{35} \gamma + \frac{848}{315} \\ \mathcal{L}_3 = \frac{512}{105} \gamma^2 - \frac{4352}{525} \gamma + \frac{13184}{4725} \\ \mathcal{L}_4 = -\frac{1024}{99} \gamma^3 + \dots \end{aligned} \quad (\text{B5})$$

with  $\epsilon^{TG} = \pi^2/3$ . The expression (B4) was obtained [50] by fitting the ground state energy to a polynomial expression in  $\sqrt{\gamma}$  for  $\gamma < 15$ . An exact expansion has been conjectured [51,52]. We have checked that in the range  $0 < \gamma < 8$  the relative difference between the two expressions was under  $2 \times 10^{-3}$ , while the relative difference between the derivatives was under  $10^{-2}$ . Using the expansion [51,52] instead of Eq. (B4) in the variational calculation of the ground state energy yields relative differences under  $5 \times 10^{-3}$ . Concerning



the expression (B5), we note that an alternative asymptotic expansion [77,78] in powers of  $1/\gamma$  also applies for  $\gamma \gg 1$ . However, the expression (B5) is more convenient [50] to match with (B4) in the intermediate region of  $\gamma \sim 1$ .

$$S(k) = \frac{k^2}{2m\omega_-(k)} \frac{{}_2F_1\left(1 + \frac{\sqrt{K}}{1+\sqrt{K}} + \mu_-(k) + \mu_+(k), 1 + \mu_-(k); 2 + \mu_-(k) - \mu_+(k), 1 - \left(\frac{\omega_-(k)}{\omega_+(k)}\right)^2\right)}{{}_2F_1\left(1 + \frac{2\sqrt{K}}{1+\sqrt{K}} + \mu_-(k) + \mu_+(k), 1 + \mu_-(k); 2 + \mu_-(k) - \mu_+(k), 1 - \left(\frac{\omega_-(k)}{\omega_+(k)}\right)^2\right)} \quad (\text{B6})$$

where  $K = 4\pi^2\rho(\pm q_0)$  is the Tomonaga-Luttinger exponent,  $\omega_+(k)$  is the dispersion of the Type-I Lieb excitations [49],  $\omega_-(k)$  the dispersion of the Type-II Lieb excitations [49] for  $k < 2\pi n$  and  $\omega_+(k - 2\pi n)$  otherwise, and  $\mu_{\pm}(k)$  are the exponents of the threshold singularity, respectively, at  $\omega_{\pm}(k)$  and can be calculated from the shift function [54,79,80]. The expression (B6) reduces to Eq. (22) in Ref. [54] when the approximation  $K \simeq 1$  is made (Fig. 10).

To calculate  $S(k)$  we have to consider [54] the integral equation for the shift function:

$$F_B(v|\lambda) - \frac{1}{2\pi} \int_{-q_0}^{q_0} \frac{2c}{(v-\mu)^2 + c^2} F_B(\mu|\lambda) d\mu = \frac{1}{2} + \frac{1}{\pi} \arctan\left(\frac{v-\lambda}{c}\right), \quad (\text{B7})$$

and

$$\omega_{p,h}(\lambda) = \pm \frac{\hbar^2}{2m} \left[ \lambda^2 - 2 \int_{-q_0}^{q_0} \mu F_B(\mu|\lambda) d\mu \right] \quad (\text{B8})$$

$$k_{p,h}(\lambda) = \pm \left[ \lambda + 2 \int_{-q_0}^{q_0} \arctan\left(\frac{\lambda-\mu}{c}\right) \rho(\mu) d\mu \right] \quad (\text{B9})$$

Then, the dispersion of Lieb modes is given by:

$$\begin{aligned} \omega_+(\lambda) &= \omega_h(q_0) + \omega_p(q_0 + \lambda) \\ k_+(\lambda) &= k_h(q_0) + k_p(q_0 + \lambda) \end{aligned} \quad (\text{B10})$$

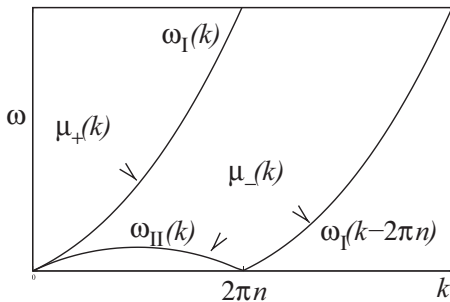


FIG. 10. Dispersion of the Lieb-I and Lieb-II modes. The dynamical structure factor is nonvanishing for  $\omega_{II}(k) < \omega < \omega_I(k)$  for  $0 < k < 2\pi n$  and  $\omega_I(k - 2\pi n) < \omega < \omega_I(k)$  for  $k > 2\pi n$ .  $\mu_+(k)$  is the threshold singularity exponent of the dynamical structure factor near the higher branch of excitations, while  $\mu_-(k)$  is the exponent near the lower branch.

Using the phenomenological suggestion given in Ref. [54] for structure factor  $S(k, \omega)$  it is possible to have an approximate estimate of the static structure factor  $S(k)$  in terms of ratio between Gauss hypergeometric functions [63]

for type I, and

$$\begin{aligned} \omega_-(\lambda) &= \omega_p(q_0) + \omega_h(q_0 - \lambda) \\ k_-(\lambda) &= k_p(q_0) + k_h(q_0 - \lambda) \end{aligned} \quad (\text{B11})$$

with  $\lambda < q_0$  for type II. When  $\lambda > q_0$ , Eq. (B11) reduces, up to a sign, to the dispersion of the Lieb-I mode shifted of  $2\pi n$ . For a given wave vector  $k$ , one must first determine  $\lambda_{\pm}(k)$  that solves  $k_{\pm}(\lambda_{\pm}) = k$  and calculate  $\omega_{\pm}(\lambda_{\pm}(k))$  to obtain the dispersion [49,54]. Once  $\lambda_+$  is known, the quantities

$$\delta_{\pm}(\lambda_+(k)) = 2\pi F_B(\pm q_0, \lambda_+(k)) \quad (\text{B12})$$

are found from the integral equation (B7), and the threshold exponent of the Lieb-I mode [79,80] is

$$\begin{aligned} \mu_+(k) &= 1 - \frac{1}{2} \left( \frac{1}{\sqrt{K}} + \frac{\delta_+(\lambda_+) - \delta_-(\lambda_+)}{2\pi} \right)^2 \\ &\quad - \frac{1}{2} \left( \frac{\delta_+(\lambda_+) + \delta_-(\lambda_+)}{2\pi} \right)^2. \end{aligned} \quad (\text{B13})$$

Similarly, having found  $\lambda_-$ , one obtains  $\delta_{\pm}(\lambda_-)$  by replacing  $\lambda_+$  with  $\lambda_-$  in (B12). Substituting  $\lambda_+$  with  $\lambda_-$  in Eq. (B13), the threshold singularity exponent  $\mu_-(k)$  of the dynamical structure factor at the lower edge is found [54,79,80]. For  $k < 2\pi n$ , the lower edge is given by the Lieb-II mode, while for  $k > 2\pi n$  it is given by a replica of the Lieb-I mode shifted by  $2\pi n$ .

In the limit of  $\gamma \rightarrow +\infty$ , the exact expression of  $S(k)$  simplifies to

$$S(k) = \frac{|k|}{2\pi n} \theta(2\pi n - |k|) + \theta(|k| - 2\pi n). \quad (\text{B14})$$

In some selected cases,  $S(k)$  from quantum Monte Carlo simulations can be used as benchmark for expression (B6); comparison between the static structure factor from simulations and from the approximated ansatz, for some selected cases, are shown in Fig. 11. The linear increase  $S(k) = \frac{K|k|}{2\pi n} + o(k)$  for small  $k$  predicted by bosonization [7] is well reproduced by both simulations and the ansatz (B6). The agreement between simulations and ansatz is better for the case of  $\gamma > 1$ . We note that in Ref. [54], a satisfactory comparison with the expression obtained for form factor summation was already shown.

### APPENDIX C: MINIMIZATION OF THE ENERGY

In Fig. 12 we show Eq. (19) with and without the dipolar interaction term, for  $a_{1D} = 5000a_0$  and  $n = 2.0 \mu\text{m}^{-1}$ , for  $\theta = 0$  when the interaction is maximally attractive and for

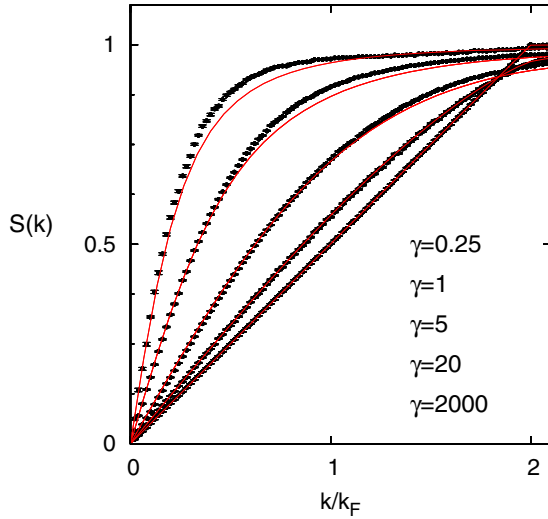


FIG. 11. Comparison of the structure factor  $S(k)$  calculated from the Cherny-Brand ansatz [54] (red solid lines) with the structure factor obtained from QuantumMonte Carlo calculations (black solid dots).  $S(k)$  is increasing linearly for low  $k$  with a slope that is a decreasing function of  $\gamma$ . For large  $k$ , it saturates to the value 1. In the figure,  $k_F = \pi n$ .

$\theta = \pi/2$  when the interaction is maximally repulsive. When the dipolar interaction is repulsive it enhances the total repulsion and hence the optimal value of  $\gamma$  is greater than  $\gamma_0$ , whereas when it is attractive it reduces the total repulsion so that the optimal  $\gamma < \gamma_0$ .

#### APPENDIX D: HIGH AND LOW DENSITY LIMITS OF THE VARIATIONAL ENERGY

Analytic expressions of  $\frac{E}{L}$  can be obtained using the Lieb-Liniger ground state energy derived in Ref. [50] and the

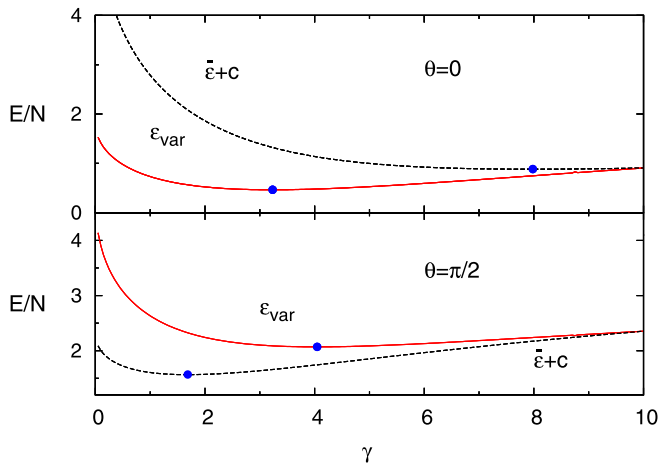


FIG. 12.  $E/N$  as a function of  $\gamma$  with (red solid line) and without the soft dipolar interaction,  $\bar{\epsilon} = \epsilon(\gamma) - \bar{\gamma} \frac{\partial \epsilon(\gamma)}{\partial \gamma}$  where we have added a constant (black dashed line). The solid blue points on the curves show the minimum of  $E/N$ . In the upper panel we show results for  $\theta = 0$  when  $V_{\text{DDI}}^{\text{ID}}$  is maximally attractive and in the lower panel we show results for  $\theta = \pi/2$  when  $V_{\text{DDI}}^{\text{ID}}$  is maximally repulsive.

expressions of the structure factor derived in Ref. [54] for  $\gamma \ll 1$  and for  $\gamma \gg 1$ . In the latter case, using (24), we have

$$\frac{E}{L} = \frac{\hbar^2 \pi^2 n^3}{6m} + \frac{\hbar^2 n^2 a_d}{m l_{\perp}^2} (1 - 3 \cos^2 \theta) + \frac{\hbar^2 a_d (1 - 3 \cos^2 \theta)}{\pi m l_{\perp}^4} \times \int_0^{2\pi n l_{\perp}} du \left( \frac{u}{2\pi} - n l_{\perp} \right) \left[ 1 - \frac{u^2}{2} e^{\frac{u^2}{2}} E_1 \left( \frac{u^2}{2} \right) \right], \quad (\text{D1})$$

and using (9) and (10) the Tomonaga-Luttinger exponent is given by

$$K^{-2} = 1 + n a_d (1 - 3 \cos^2 \theta) e^{\frac{(2\pi n l_{\perp})^2}{2}} E_1 \left( \frac{(2\pi n l_{\perp})^2}{2} \right), \quad (\text{D2})$$

so that in the limit  $n l_{\perp} \rightarrow 0$ ,  $K = 1 + n a_d (1 - 3 \cos^2 \theta) \ln(\pi \sqrt{2} e^{\gamma/2} n l_{\perp}) + O(n^3)$ , the expected behavior with interactions decaying as  $1/|x|^3$  at long distance. In the case of  $\gamma \ll 1$ , we can approximate [54]

$$S(k) \simeq \frac{|k|}{\sqrt{k^2 + 4\gamma n^2}}, \quad (\text{D3})$$

leading to a variational energy

$$\frac{E}{L} \simeq \frac{\hbar^2 n^3}{2m} \left[ \epsilon(\gamma) - \bar{\gamma} \frac{\partial \epsilon}{\partial \gamma} \right] + V(\theta) \left[ 2n^2 l_{\perp} - n \sqrt{\frac{\pi}{2}} + \frac{n}{2\pi} \int_0^{+\infty} \frac{1 - u e^u E_1(u)}{\sqrt{2u + 4\gamma n^2 l_{\perp}^2}} du \right]. \quad (\text{D4})$$

Minimizing with respect to  $\bar{\gamma}$ , we obtain

$$\frac{\partial}{\partial \gamma} \left( \frac{E}{L} \right) \simeq -\frac{\hbar^2 n^3}{2m} \bar{\gamma} \epsilon''(\gamma) + \frac{n}{2\pi} \frac{dI}{d\gamma}(\gamma) = 0, \quad (\text{D5})$$

where we have defined

$$I(\gamma) = \int_0^{+\infty} \frac{1 - u e^u E_1(u)}{\sqrt{2u + 4\gamma n^2 l_{\perp}^2}} du. \quad (\text{D6})$$

According to Eq. (7), for  $n \rightarrow +\infty$ ,  $\gamma n^2 \rightarrow +\infty$ , so we can replace the denominator in the integral  $I(\gamma)$  with  $(4\gamma n^2 l_{\perp}^2)^{3/2}$ . Using the expansion [50] of  $\epsilon(\gamma)$  valid for  $\gamma \ll 1$ , we end up with

$$\bar{\gamma} \simeq \sqrt{2\pi} \frac{\hbar^2 a_d (1 - 3 \cos^2 \theta)}{m g n^2 l_{\perp}^4}, \quad (\text{D7})$$

so  $\bar{g} = O(n^{-1})$  when  $n \rightarrow +\infty$ . In the high density limit,  $\gamma \rightarrow \gamma_0$ , and the leading order expansion is

$$g = g_{\text{vdW}} - \frac{\hbar^2 a_d (1 - 3 \cos^2 \theta)}{2m l_{\perp}^2} \times \left[ \frac{8}{3} - \sqrt{\frac{\pi}{2}} \frac{1}{n a_d \left( \frac{4l_{\perp}^2}{|a_d| |a_{\text{ID}}|} - \frac{8}{3} (1 - 3 \cos^2 \theta) \right)} + \dots \right]. \quad (\text{D8})$$

This behavior is illustrated in Fig. 1.

- [1] M. A. Cazalilla, R. Citro, T. Giamarchi, E. Orignac, and M. Rigol, *Rev. Mod. Phys.* **83**, 1405 (2011).
- [2] F. D. M. Haldane, *Phys. Rev. Lett.* **47**, 1840 (1981).
- [3] T. Giamarchi, *Quantum Physics in One Dimension* (Oxford University Press, Oxford, 2004).
- [4] E. H. Lieb and W. Liniger, *Phys. Rev.* **130**, 1605 (1963).
- [5] L. Amico and V. Korepin, *Ann. Phys. (NY)* **314**, 496 (2004).
- [6] F. Mazzanti, G. E. Astrakharchik, J. Boronat, and J. Casulleras, *Phys. Rev. A* **77**, 043632 (2008).
- [7] R. Citro, E. Orignac, S. De Palo, and M.-L. Chiofalo, *Phys. Rev. A* **75**, 051602(R) (2007).
- [8] T. D. Kühner and H. Monien, *Phys. Rev. B* **58**, R14741 (1998).
- [9] C. S. Hellberg and E. J. Mele, *Phys. Rev. Lett.* **67**, 2080 (1991).
- [10] N. Kawakami and P. Horsch, *Phys. Rev. Lett.* **68**, 3110 (1992).
- [11] C. S. Hellberg and E. J. Mele, *Phys. Rev. Lett.* **68**, 3111 (1992).
- [12] E. Fradkin, E. Moreno, and F. A. Schaposnik, *Nucl. Phys. B* **392**, 667 (1993).
- [13] K. V. Pham, M. Gabay, and P. Lederer, *Phys. Rev. B* **61**, 16397 (2000).
- [14] F. Calogero, *J. Math. Phys.* **10**, 2191 (1969).
- [15] F. Calogero, *J. Math. Phys.* **10**, 2197 (1969).
- [16] B. Sutherland, *J. Math. Phys.* **12**, 246 (1971).
- [17] B. Sutherland, *J. Math. Phys.* **12**, 251 (1971).
- [18] B. Sutherland, *Phys. Rev. A* **4**, 2019 (1971).
- [19] M. Capello, F. Becca, M. Fabrizio, and S. Sorella, *Phys. Rev. Lett.* **99**, 056402 (2007).
- [20] R. Jastrow, *Phys. Rev.* **98**, 1479 (1955).
- [21] D. Rubeni, A. Foerster, and I. Roditi, *Phys. Rev. A* **86**, 043619 (2012).
- [22] B. Wilson, A. Foerster, C. Kuhn, I. Roditi, and D. Rubeni, *Phys. Lett. A* **378**, 1065 (2014).
- [23] G. Xianlong, M. Polini, M. P. Tosi, V. L. Campo, Jr., K. Capelle, and M. Rigol, *Phys. Rev. B* **73**, 165120 (2006).
- [24] S. Schenk, M. Dzierzawa, P. Schwab, and U. Eckern, *Phys. Rev. B* **78**, 165102 (2008).
- [25] J.-S. Caux and J.-M. Maillet, *Phys. Rev. Lett.* **95**, 077201 (2005).
- [26] J.-S. Caux and P. Calabrese, *Phys. Rev. A* **74**, 031605(R) (2006).
- [27] P. W. Claeys, J.-S. Caux, D. Van Neck, and S. De Baerdemacker, *Phys. Rev. B* **96**, 155149 (2017).
- [28] M. Lu, N. Q. Burdick, S. H. Youn, and B. L. Lev, *Phys. Rev. Lett.* **107**, 190401 (2011).
- [29] M. Lu, N. Q. Burdick, and B. L. Lev, *Phys. Rev. Lett.* **108**, 215301 (2012).
- [30] K. Aikawa, A. Frisch, M. Mark, S. Baier, A. Rietzler, R. Grimm, and F. Ferlino, *Phys. Rev. Lett.* **108**, 210401 (2012).
- [31] K. Aikawa, A. Frisch, M. Mark, S. Baier, R. Grimm, and F. Ferlino, *Phys. Rev. Lett.* **112**, 010404 (2014).
- [32] H. Kadau, M. Schmitt, M. Wenzel, C. Wink, T. Maier, I. Ferrier-Barbut, and T. Pfau, *Nature (London)* **530**, 194 (2016).
- [33] L. Chomaz, S. Baier, D. Petter, M. J. Mark, F. Wächtler, L. Santos, and F. Ferlino, *Phys. Rev. X* **6**, 041039 (2016).
- [34] I. Ferrier-Barbut, H. Kadau, M. Schmitt, M. Wenzel, and T. Pfau, *Phys. Rev. Lett.* **116**, 215301 (2016).
- [35] A. de Paz, A. Sharma, A. Chotia, E. Maréchal, J. H. Huckans, P. Pedri, L. Santos, O. Gorceix, L. Vernac, and B. Laburthe-Tolra, *Phys. Rev. Lett.* **111**, 185305 (2013).
- [36] A. de Paz, P. Pedri, A. Sharma, M. Efremov, B. Naylor, O. Gorceix, E. Maréchal, L. Vernac, and B. Laburthe-Tolra, *Phys. Rev. A* **93**, 021603(R) (2016).
- [37] S. Baier, M. J. Mark, D. Petter, K. Aikawa, Z. C. L. Chomaz, M. Baranov, P. Zoller, and F. Ferlino, *Science* **352**, 201 (2016).
- [38] B. Naylor, M. Brewczyk, M. Gajda, O. Gorceix, E. Marechal, L. Vernac, and B. Laburthe-Tolra, *Phys. Rev. Lett.* **117**, 185302 (2016).
- [39] Y. Tang, W. Kao, K.-Y. Li, S. Seo, K. Mallayya, M. Rigol, S. Gopalakrishnan, and B. L. Lev, *Phys. Rev. X* **8**, 021030 (2018).
- [40] S. Sinha and L. Santos, *Phys. Rev. Lett.* **99**, 140406 (2007).
- [41] S. Yi, T. Li, and C. P. Sun, *Phys. Rev. Lett.* **98**, 260405 (2007).
- [42] M. Hafezi, A. S. Sørensen, E. Demler, and M. D. Lukin, *Phys. Rev. A* **76**, 023613 (2007).
- [43] M. Fattori, G. Roati, B. Deissler, C. D'Errico, M. Zaccanti, M. Jona-Lasinio, L. Santos, M. Inguscio, and G. Modugno, *Phys. Rev. Lett.* **101**, 190405 (2008).
- [44] K. W. Wilsmann, L. H. Ymai, A. P. Tonel, J. Links, and A. Foerster, *Commun. Phys.* **1**, 91 (2018).
- [45] A. S. Arkhipov, G. E. Astrakharchik, A. V. Belikov, and Y. E. Lozovik, *JETP Lett.* **82**, 39 (2005).
- [46] R. Citro, S. De Palo, E. Orignac, P. Pedri, and M. Chiofalo, *New J. Phys.* **10**, 045011 (2008).
- [47] M. Girardeau, *J. Math. Phys.* **1**, 516 (1960).
- [48] F. Deuretzbacher, J. C. Cremon, and S. M. Reimann, *Phys. Rev. A* **81**, 063616 (2010); **87**, 039903(E) (2013).
- [49] E. H. Lieb, *Phys. Rev.* **130**, 1616 (1963).
- [50] G. Lang, F. Hekking, and A. Minguzzi, *SciPost Phys.* **3**, 003 (2017).
- [51] Z. Ristivojevic, *Phys. Rev. B* **100**, 081110(R) (2019).
- [52] M. Marino and T. Reis, *J. Stat. Phys.* **177**, 1148 (2019).
- [53] G. E. Astrakharchik and S. Giorgini, *Phys. Rev. A* **68**, 031602(R) (2003).
- [54] A. Y. Cherny and J. Brand, *Phys. Rev. A* **79**, 043607 (2009).
- [55] E. Haller, R. Hart, M. J. Mark, J. G. Danzl, L. Reichsöllner, M. Gustavsson, M. Dalmonte, G. Pupillo, and H.-C. Nägerl, *Nature (London)* **466**, 597 (2010).
- [56] M. Dalmonte, G. Pupillo, and P. Zoller, *Phys. Rev. Lett.* **105**, 140401 (2010).
- [57] G. Boéris, L. Gori, M. D. Hoogerland, A. Kumar, E. Lucioni, L. Tanzi, M. Inguscio, T. Giamarchi, C. D'Errico, G. Carleo, G. Modugno, and L. Sanchez-Palencia, *Phys. Rev. A* **93**, 011601(R) (2016).
- [58] M. Nakamura and K. Nomura, *Phys. Rev. B* **56**, 12840 (1997).
- [59] D. C. Cabra and J. E. Drut, *J. Phys.: Condens. Matter* **15**, 1445 (2003).
- [60] K. Huang and C. N. Yang, *Phys. Rev.* **105**, 767 (1957).
- [61] M. Olshanii, *Phys. Rev. Lett.* **81**, 938 (1998).
- [62] T. Shi and S. Yi, *Phys. Rev. A* **90**, 042710 (2014).
- [63] Edited by M. Abramowitz and I. Stegun, *Handbook of Mathematical Functions* (Dover, New York, 1972).
- [64] Y. Tang, A. Sykes, N. Q. Burdick, J. L. Bohn, and B. L. Lev, *Phys. Rev. A* **92**, 022703 (2015).
- [65] W. H. Press, S. A. Teukolsky, W. T. Vetterling, and B. P. Flannery, *Numerical Recipes in Fortran : The Art of Scientific Computing* (Cambridge University Press, Cambridge, 1992), Chap. 10, p. 390.
- [66] S. De Palo, E. Orignac, R. Citro, and M. L. Chiofalo, *Phys. Rev. B* **77**, 212101 (2008).

- [67] T. Roscilde and M. Boninsegni, *New J. Phys.* **12**, 033032 (2010).
- [68] C. Menotti and S. Stringari, *Phys. Rev. A* **66**, 043610 (2002).
- [69] J. N. Fuchs, X. Leyronas, and R. Combescot, *Phys. Rev. A* **68**, 043610 (2003).
- [70] J. N. Fuchs, X. Leyronas, and R. Combescot, *Laser Phys.* **14**, 551 (2004).
- [71] R. Ołdziejewski, W. Górecki, K. Pawłowski, and K. Rzążewski, Strongly correlated quantum droplets in quasi-1D dipolar Bose gas (2019), [arXiv:1908.00108](https://arxiv.org/abs/1908.00108).
- [72] M. Mattioli, M. Dalmonte, W. Lechner, and G. Pupillo, *Phys. Rev. Lett.* **111**, 165302 (2013).
- [73] J. S. Douglas, H. Habibian, C. L. Hung, A. V. Gorshkov, H. J. Kimble, and D. E. Chang, *Nat. Photonics* **9**, 326 (2015).
- [74] R. P. Feynman, *Statistical Mechanics* (Benjamin, Reading, MA, 1972).
- [75] C. N. Yang and C. P. Yang, *J. Math. Phys.* **10**, 1115 (1969).
- [76] M. Panfil and J.-S. Caux, *Phys. Rev. A* **89**, 033605 (2014).
- [77] Z. Ristivojevic, *Phys. Rev. Lett.* **113**, 015301 (2014).
- [78] G. Lang, *SciPost Phys.* **7**, 55 (2019).
- [79] M. Khodas, M. Pustilnik, A. Kamenev, and L. I. Glazman, *Phys. Rev. Lett.* **99**, 110405 (2007).
- [80] A. Imambekov and L. I. Glazman, *Phys. Rev. Lett.* **102**, 126405 (2009).